ALEA, Lat. Am. J. Probab. Math. Stat. **18**, 167–192 (2021)
DOI: 10.30757/ALEA.v18-08

Simulations for Karlin random fields

Zuopeng Fu and Yizao Wang

Department of Mathematical Sciences
University of Cincinnati
2815 Commons Way
Cincinnati, OH, 45221-0025, USA.
E-mail address: fuzg@mail.uc.edu , yizao.wang@uc.edu

Abstract. We investigate the simulation methods for a large family of stable random fields that appeared in the recent literature, known as the Karlin stable set-indexed processes. We exploit a new representation and implement the procedure introduced by Asmussen and Rosiński (2001) by first decomposing the random fields into large-jump and small-jump parts, and simulating each part separately. As special cases, simulations for several manifold-indexed processes are considered, and adjustments are introduced accordingly in order to improve the computational efficiency.

1. Introduction

This paper is a continuation of our earlier work on Karlin stable set-indexed processes in Fu and Wang (2020). In the most general framework, a Karlin stable set-indexed process is associated to a measure space $(E, \mathcal{E}, \mu)$ with a σ-finite measure μ and an index set $\mathcal{A} \subset \mathcal{E}$ such that for each $A \in \mathcal{A}$, $\mu(A) < \infty$. Fix $(E, \mathcal{E}, \mu)$ and $\mathcal{A}$. Then, the corresponding Karlin stable set-indexed process, denoted by $Y_{\alpha,\beta}$ for $\alpha \in (0, 2]$ and $\beta \in (0, 1)$, is defined via the following stochastic-integral representation (Fu and Wang, 2020, Remark 3.2)

$$\{Y_{\alpha,\beta}(A)\}_{A\in\mathcal{A}} \stackrel{d}{=} \left\{\int_{\mathbb{R}_+\times\Omega'} \mathbf{1}_{\{[\mathcal{N}'^{(r)}(\omega')](A) \text{ odd}\}} M_\alpha(drd\omega')\right\}_{A\in\mathcal{A}}, \tag{1.1}$$

where $(\Omega', \mathcal{F}', \mathbb{P}')$ is another probability space, on which $\mathcal{N}'^{(r)}$ is a Poisson point process on $(E, \mathcal{E})$ with intensity measure $r\mu$, $r > 0$, M_α is an SαS random measure

Received by the editors April 10th, 2020; accepted October 27th, 2020.
2010 *Mathematics Subject Classification.* 60G22, 60G52; Secondary, 60G60.
Key words and phrases. Lévy–Chentsov stable field, set-indexed process, simulation, stable process, infinitely-divisible process.

on $\mathbb{R}_+ \times \Omega'$ with control measure $c_\beta r^{-\beta-1} dr d\mathbb{P}'$, and

$$c_\beta := \frac{\beta 2^{1-\beta}}{\Gamma(1-\beta)}.$$

We shall refer to a Karlin stable set-indexed process as a Karlin random field in short from time to time, and its law is throughout understood in their finite-dimensional distributions (so is the notation '$\stackrel{d}{=}$'). The constant c_β is chosen so that $\mathbb{E}\exp(i\theta Y_{\alpha,\beta}(A)) = \exp\left(-\mu^\beta(A)|\theta|^\alpha\right), \alpha \in (0,2)$. Recent developments on the Karlin random fields include Durieu and Wang (2016); Durieu et al. (2020), based on the original work of Karlin (1967). The Karlin model is an infinite urn model that plays a fundamental role in combinatorial stochastic processes (Pitman, 2006; Gnedin et al., 2007).

The abstract representation (1.1) of Karlin random fields provides a stochastic-integral representation for set-indexed fractional Brownian motions ($\alpha = 2$, see Lemma 2.3 below) (Herbin and Merzbach, 2006) and hence extends set-indexed fractional Brownian motions to stable cases. It has a few notable manifold-indexed examples as summarized below. When $\alpha = 2$, these are well-investigated centered Gaussian random fields, with the covariance functions recalled respectively.

(i) Karlin stable processes, with

$$(E, \mathcal{E}, \mu) = (\mathbb{R}_+, \mathcal{B}(\mathbb{R}_+), \mathrm{Leb}), \text{ and } \{A_t\}_{t\geqslant 0} = \{[0,t]\}_{t\geqslant 0}.$$

When $\alpha = 2$, these are fractional Brownian motions with Hurst index $\beta/2 \in (0,1)$, with covariance function

$$\frac{1}{2}\left(s^\beta + t^\beta - |s-t|^\beta\right), s,t \geqslant 0. \tag{1.2}$$

(ii) Multiparameter fractional stable fields, with

$$(E, \mathcal{E}, \mu) = (\mathbb{R}_+^2, \mathcal{B}(\mathbb{R}_+^2), \mathrm{Leb}), \text{ and } \{A_{\boldsymbol{t}}\}_{\boldsymbol{t}\in\mathbb{R}_+^2} = \{[\boldsymbol{0}, \boldsymbol{t}]\}_{\boldsymbol{t}\in\mathbb{R}_+^2}.$$

When $\alpha = 2$, these are multiparameter fractional Brownian motions introduced in Herbin and Merzbach (2007), with covariance function

$$\frac{1}{2}\left(\mathrm{Leb}([\boldsymbol{0},\boldsymbol{s}])^\beta + \mathrm{Leb}([\boldsymbol{0},\boldsymbol{t}])^\beta - \mathrm{Leb}([\boldsymbol{0},\boldsymbol{s}]\Delta[\boldsymbol{0},\boldsymbol{t}])^\beta\right), \boldsymbol{s},\boldsymbol{t} \geqslant 0. \tag{1.3}$$

We write $[\boldsymbol{a}, \boldsymbol{b}] = [a_1, b_1] \times [a_2, b_2]$ for $\boldsymbol{a} = (a_1, a_2), \boldsymbol{b} = (b_1, b_2) \in \mathbb{R}_+^2$.

(iii) Fractional Lévy–Chentsov stable fields, with

$$(E, \mathcal{E}, \mu) = \left(\mathbb{S}^1 \times \mathbb{R}_+, \mathcal{B}(\mathbb{S}^1 \times \mathbb{R}_+), d\boldsymbol{s}dr\right),$$

where $d\boldsymbol{s}dr$ is the product measure of the uniform measure $d\boldsymbol{s}$ on $\mathbb{S}^1$ and the Lebesgue measure dr on $\mathbb{R}_+$, and

$$A_{\boldsymbol{t}} = \left\{(\boldsymbol{s}, r) : \boldsymbol{s} \in \mathbb{S}^1, 0 < r < \langle \boldsymbol{s}, \boldsymbol{t}\rangle\right\}, \boldsymbol{t} \in \mathbb{R}^2.$$

This family and the one in the next examples extend the well-known Lévy–Chentsov stable fields (Samorodnitsky and Taqqu, 1994; Takenaka, 2010). With $\alpha = 2$, these are the fractional Lévy Brownian fields with Hurst index $\beta/2 \in (0,1)$ (Samorodnitsky and Taqqu, 1994), with covariance function

$$\frac{1}{2}\left(\|\boldsymbol{s}\|_2^\beta + \|\boldsymbol{t}\|_2^\beta - \|\boldsymbol{t}-\boldsymbol{s}\|_2^\beta\right), \boldsymbol{s},\boldsymbol{t} \in \mathbb{R}^2. \tag{1.4}$$

(iv) Spherical fractional Lévy–Chenstov stable fields, with

$$(E, \mathcal{E}, \mu) = (\mathbb{S}^2, \mathcal{B}(\mathbb{S}^2), d\boldsymbol{s}),$$

where $d\boldsymbol{s}$ is the Lebesgue measure on the unit sphere $\mathbb{S}^2$ in $\mathbb{R}^3$, and

$$A_{\boldsymbol{x}} = H_{\boldsymbol{x}} \triangle H_{\boldsymbol{o}}, \boldsymbol{x} \in \mathbb{S}^2 \quad \text{with} \quad H_{\boldsymbol{x}} := \left\{ \boldsymbol{y} \in \mathbb{S}^2 : \langle \boldsymbol{x}, \boldsymbol{y} \rangle > 0 \right\},$$

where $\boldsymbol{o} \in \mathbb{S}^2$ is an arbitrary fixed point. When $\alpha = 2$, these are spherical fractional Brownian motions with Hurst index $\beta/2 \in (0,1)$ (Istas, 2005), with covariance function ($\mathsf{d}_{\mathbb{S}^2}$ is the geodesic metric on $\mathbb{S}^2$)

$$\frac{1}{2}\left(\mathsf{d}_{\mathbb{S}^2}^{\beta}(\boldsymbol{o}, \boldsymbol{x}) + \mathsf{d}_{\mathbb{S}^2}^{\beta}(\boldsymbol{o}, \boldsymbol{y}) - \mathsf{d}_{\mathbb{S}^2}^{\beta}(\boldsymbol{x}, \boldsymbol{y}) \right), \boldsymbol{x}, \boldsymbol{y} \in \mathbb{S}^2.$$

In this paper we investigate the corresponding simulation methods. Simulation methods for Gaussian random fields have been extensively studied in theory and broadly applied in various fields (see e.g. Biermé, 2019; Cohen and Istas, 2013; Kroese and Botev, 2015 for overviews, and Gelbaum and Titus, 2014; van Wyk et al., 2015 for some recent attempts for models with more general manifold index sets). As for stable processes and more generally infinitely-divisible processes, the foundation of simulation methods has been laid down in the seminal work of Asmussen and Rosiński (2001). They focused on Lévy processes in the original paper, but essentially the same idea applies to more general stable processes and infinitely-divisible processes, carried out in details by Lacaux and coauthors later (Lacaux, 2004a,b; Cohen et al., 2008). These references served as our starting point. Namely, it has been well understood since then that in order to simulate an infinitely-divisible process, in practice one should first decompose the process into two independent components consisting of large and small jumps respectively, and then simulate each part separately. We shall follow the same idea here for the Karlin random fields (see Remark A.3 for subtile differences between our framework and aforementioned ones), and the two parts are referred to as the large-jump and small-jump parts, respectively.

The main contribution of this paper is two-folded.

(a) First, we develop a new representation for Karlin random fields, *when restricted to a bounded domain*: that is, the index set $\mathcal{A}_0$ is such that there exists $E_0 \in \mathcal{E}$ with $\mu(E_0) < \infty$ and for all $A \in \mathcal{A}_0$, $A \subset E_0$ (Theorem 2.1). All the examples mentioned above, when simulated over a bounded domain, can be reduced to such a situation and hence the new representation applies. The advantage of this new representation is that it provides a compound–Poisson representation for the large-jump part in the Asmussen–Rosiński approach, and hence yields immediately an exact and straightforward simulation method for this part. This is in contrast to the developments in Lacaux (2004a,b); Cohen et al. (2008), where for most interesting examples the simulations for the large-jump part require approximation methods.

(b) We then apply the new representation to the aforementioned examples, and propose adjustments accordingly in order to improve computational efficiency. Most notably, a straightforward implementation of the Asmussen–Rosiński approach would meet computational issues even in the simplest case of $\mathbb{R}_+$-indexed Karlin stable processes. The issues are due to the fact that the new representation is essentially based on the so-called *odd-occupancy vector*, the law of which is determined by the β-Sibuya distribution (of which the tail is regularly varying with index $-\beta$, $\beta \in (0,1)$). Sampling directly from the heavy-tailed Sibuya distribution is very inefficient in practice, and in a couple situations we managed to propose a computational efficient method to sample the odd-occupancy vector directly without sampling the Sibuya distribution.

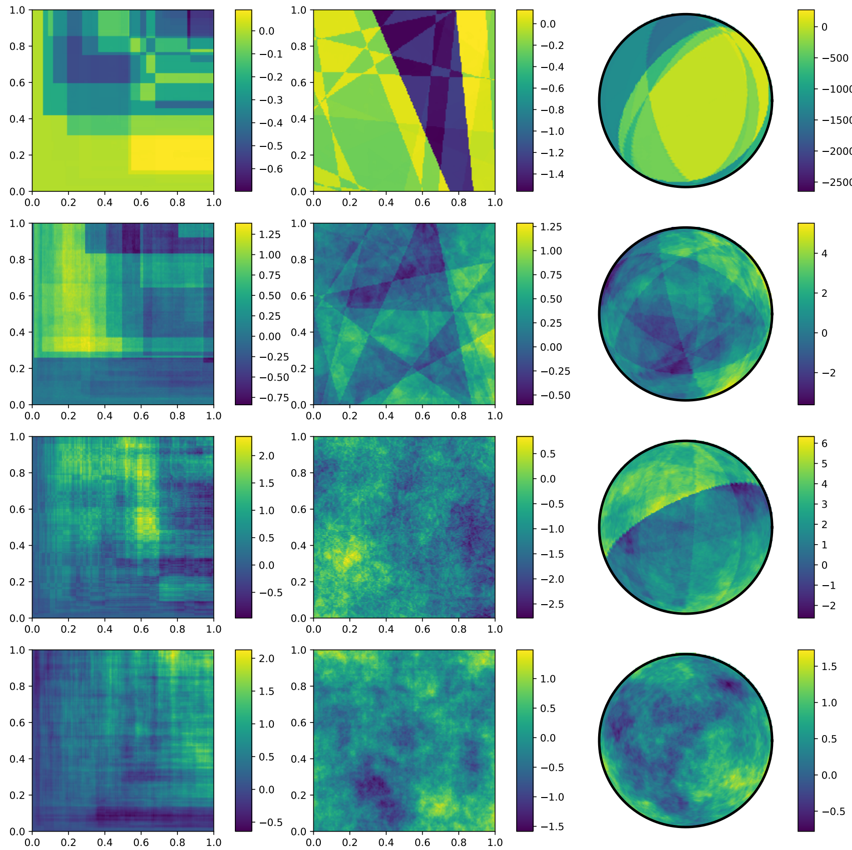

FIGURE 1.1. Simulations for $\mathbb{R}^2_+$-indexed multiparameter fractional stable fields (left), $\mathbb{R}^2$-indexed fractional Lévy–Chentsov stable fields (middle) and $\mathbb{S}^2$-indexed fractional Lévy–Chentsov stable fields (right), with $\alpha = 0.5$ (top) $\alpha = 1.2$ (second row), $\alpha = 1.8$ (third row) and $\alpha = 2$ (bottom, Gaussian), and all with $\beta = 0.8$. The Gaussian cases correspond to multiparameter fractional Brownian motions, fractional Lévy Brownian fields, and spherical fractional Brownian motions, respectively.

In Figure 1.1 we provide a few simulation examples of the processes of our interest. Note that when $\alpha < 2$ these are only approximated samplings. Curiously, for fractional Lévy–Chentsov stable fields, the odd-occupancy vectors are functionals of models from stochastic geometry (Lantuéjoul, 2002; Schneider and Weil, 2008), as illustrated in Figures 3.7 and 3.9 later. So fractional Lévy–Chentsov stable fields can be thought of aggregations of models from stochastic geometry.

The paper is organized as follows. Section 2 introduces a new representation for the Karlin random fields, and explains the general strategy for simulations. Section 3 investigates a few examples and explains how improvement can be made regarding efficiency of the simulations. Appendix A provides a review on the general framework of Asmussen and Rosiński (2001) applied to stable processes.

2. Karlin stable set-indexed processes

2.1. *A new representation.* We develop a new representation of Karlin stable set-indexed processes, when restricted to a bounded domain. More precisely, fix some $E_0 \in \mathcal{E}$ with $\mu(E_0) < \infty$ and consider an index set $\mathcal{A}_0$ such that $A \subset E_0$ for all $A \in \mathcal{A}_0$. We let Q_β be a random variable with the Sibuya distribution with parameter $\beta \in (0,1)$, determined by $\mathbb{E}z^{Q_\beta} = 1-(1-z)^\beta$ for all $z \in [0,1]$ (Sibuya, 1979). Equivalently, Q_β takes values from $\mathbb{N}$ with

$$\mathbb{P}(Q_\beta = k) = \frac{\beta}{\Gamma(1-\beta)}\frac{\Gamma(k-\beta)}{\Gamma(k+1)} \sim \frac{\beta}{\Gamma(1-\beta)}k^{-1-\beta} \text{ as } k \to \infty,$$

so it is a heavy-tailed distribution without finite β-th moment. Throughout, the following random closed set R_β in $\mathcal{F}_0(E_0)$, the space of non-empty closed subsets of E_0 (see Molchanov, 2017 for background on random closed sets), plays a fundamental role for the Karlin random fields

$$R_\beta := \bigcup_{i=1}^{Q_\beta}\{U_i\}, \tag{2.1}$$

where $\{U_i\}_{i\in\mathbb{N}}$ are i.i.d. random elements from E_0 with the law $\mu_{E_0}(\cdot) := \mu(\cdot \cap E_0)/\mu(E_0)$ independent from Q_β introduced before. So R_β is a random closed set taking values in $\mathcal{F}_0(E_0)$. The new representation is summarized as follows.

Theorem 2.1. *Assume E_0 and $\mathcal{A}_0$ as above. For all $\alpha \in (0,2]$, $\beta \in (0,1)$, the Karlin set-indexed stable process (1.1) restricted to $\mathcal{A}_0$ has the stochastic-integral representation*

$$\{Y_{\alpha,\beta}(A)\}_{A\in\mathcal{A}_0} \overset{d}{=} \left\{\int_{\Omega'} \mathbf{1}_{\{|R'_\beta(\omega')\cap A| \text{ odd}\}}\widetilde{M}_\alpha(d\omega')\right\}_{A\in\mathcal{A}_0}, \tag{2.2}$$

where $(\Omega',\mathcal{F}',\mathbb{P}')$ is another probability space, on which $R'_\beta(\omega)$ is a random element in E_0 with the same law as R_β, and $\widetilde{M}_\alpha$ is an $S\alpha S$ random measure on Ω' with control measure $2^{1-\beta}\mu^\beta(E_0)\cdot\mathbb{P}'$.

Proof: We compute the characteristic function of finite-dimensional distributions. For $d \in \mathbb{N}$, $A_1,\dots,A_d \in \mathcal{A}_0$ and $\theta_1,\dots,\theta_d \in \mathbb{R}$, we have

$$\mathbb{E}\exp\left(i\sum_{j=1}^d \theta_j Y_{\alpha,\beta}(A_j)\right) = \exp\left(-\int_{\mathbb{R}_+\times\Omega'}\left|\sum_{j=1}^d \theta_j \mathbf{1}_{\{\mathcal{N}'^{(r)}(A_j) \text{ odd}\}}\right|^\alpha c_\beta r^{-\beta-1}d\mathbb{P}'\right).$$

Note that by the property of Poisson point processes, there exists a measure $\widetilde{\nu}$ on $\mathbb{N}$ such that the above is the same as, with $\{U'_i\}_{i\in\mathbb{N}}$ as i.i.d. random variables with law μ_{E_0} (defined on some probability space denoted by $(\Omega',\mathcal{F}',\mathbb{P}')$ without loss of generality),

$$\exp\left(-\sum_{k=1}^\infty\int_{\Omega'}\left|\sum_{j=1}^d \theta_j \mathbf{1}_{\{|\bigcup_{i=1}^k\{U'_i\}\cap A_j| \text{ odd}\}}\right|^\alpha \widetilde{\nu}(\{k\})d\mathbb{P}'\right). \tag{2.3}$$

The values of $\widetilde{\nu}$ can be computed as

$$\begin{aligned}\widetilde{\nu}(\{k\}) &= c_\beta \int_0^\infty r^{-\beta-1}\mathbb{P}\left(\mathcal{N}^{(r)}(E_0)=k\right)dr = c_\beta\int_0^\infty r^{-\beta-1}\frac{(r\mu(E_0))^k}{k!}e^{-r\mu(E_0)}dr\\ &= \frac{\beta 2^{1-\beta}}{\Gamma(1-\beta)}\cdot\mu^\beta(E_0)\cdot\frac{\Gamma(k-\beta)}{\Gamma(k+1)} = 2^{1-\beta}\mu^\beta(E_0)\mathbb{P}(Q_\beta=k), \text{ for all } k\in\mathbb{N}.\end{aligned}$$

Then, (2.3) becomes, letting Q'_β be a β-Sibuya random variable on $(\Omega',\mathcal{F}',\mathbb{P}')$, independent from $\{U'_i\}_{i\in\mathbb{N}}$,

$$\begin{aligned}&\exp\left(-2^{1-\beta}\mu^\beta(E_0)\int_{\Omega'}\left|\sum_{j=1}^d\theta_j\mathbf{1}_{\left\{\left|\bigcup_{i=1}^{Q'_\beta}\{U'_i\}\cap A_j\right|\ \mathrm{odd}\right\}}\right|^\alpha d\mathbb{P}'\right)\\ &\qquad\qquad = \exp\left(-2^{1-\beta}\mu^\beta(E_0)\int_{\Omega'}\left|\sum_{j=1}^d\theta_j\mathbf{1}_{\left\{\left|R'_\beta\cap A_j\right|\ \mathrm{odd}\right\}}\right|^\alpha d\mathbb{P}'\right).\end{aligned}$$

This completes the proof. □

Remark 2.2. Let $P_{\mathcal{N}^{(r)},+}$ denote the induced probability measure of $\mathcal{N}^{(r)}$ (as a random closed set) restricted to $\mathcal{F}_0(E_0)$; in particular $P_{\mathcal{N}^{(r)},+}$ is a sub-probability measure for all $r>0$ (i.e. $P_{\mathcal{N}^{(r)},+}(\mathcal{F}_0(E_0))<1$). Let P_{R_β} denote the induced probability measure on $\mathcal{F}_0(E_0)$ by R_β. We have essentially proved

$$P_{R_\beta}(\cdot) = \frac{\beta}{\Gamma(1-\beta)\mu^\beta(E_0)}\int_0^\infty r^{-\beta-1}P_{\mathcal{N}^{(r)},+}(\cdot)dr \tag{2.4}$$

as a probability measure on $\mathcal{F}_0(E_0)$. The right-hand side, in the language of Radon point measures instead of random closed sets, appeared in Fu and Wang (2020, Eq.(3.1)) as $\mu_\beta(\cdot)/(2^{1-\beta}\mu^\beta(E_0))$ and played a central role in the representations of Karlin random fields therein.

The integral representations (2.2) with $\alpha=2$ correspond to *set-indexed fractional Brownian motions* with Hurst index $H=\beta/2\in(0,1/2)$ (Herbin and Merzbach, 2006). These are centered Gaussian processes, denoted by $\{\mathbb{B}_\mu^{\beta/2}(A)\}_{A\in\mathcal{A}_0}$, with

$$\mathrm{Cov}\left(\mathbb{B}_\mu^{\beta/2}(A_1),\mathbb{B}_\mu^{\beta/2}(A_2)\right) = \frac12\left(\mu^\beta(A_1)+\mu^\beta(A_2)-\mu^\beta(A_1\Delta A_2)\right), A_1,A_2\in\mathcal{A}_0. \tag{2.5}$$

Lemma 2.3. *Let $Y_{2,\beta}$ be as in (2.2). Then,*

$$\{Y_{2,\beta}(A)\}_{A\in\mathcal{A}_0} \stackrel{d}{=} \left\{\mathbb{B}_\mu^{\beta/2}(A)\right\}_{A\in\mathcal{A}_0}.$$

A stronger result, including a decomposition of set-indexed fractional Brownian motions, was already proved in Fu and Wang (2020, Section 3.3). We include a quick proof for a weaker result here, and we shall need the computation (2.6) below later.

Remark 2.4. Note that our covariance formula differs from the one in Fu and Wang (2020, Section 3.3) by a factor of 2. This is because therein for a streamlined presentation we took the convention that the characteristic function for a stochastic integral is $\mathbb{E}\exp(i\theta\int_S fdM_\alpha) = \exp\left(-|\theta|^\alpha\int_S|f|^\alpha d\mu\right)$ *for all* $\alpha\in(0,2]$. With $\alpha=2$ this is different from the common convention (considered above) under which the characteristic function is $\exp\left(-(1/2)|\theta|^2\int_S|f|^2d\mu\right)$ instead (e.g. Fu and Wang, 2020, Remark 2.9).

Proof of Lemma 2.3: We compute

$$\mathrm{Cov}\left(Y_{2,\beta}(A_1), Y_{2,\beta}(A_2)\right) = 2^{1-\beta}\mu^\beta(E_0)\cdot \mathbb{P}\left(R_\beta(A_1)\ \mathrm{odd}, R_\beta(A_2)\ \mathrm{odd}\right).$$

We shall use the identity (2.4) instead of using the representation (2.1) involving Q_β. Namely,

$$\begin{aligned}&\mathbb{P}\left(|R_\beta\cap A_1|\ \mathrm{odd}, |R_\beta\cap A_2|\ \mathrm{odd}\right)\\ &\qquad = \frac{\beta}{\Gamma(1-\beta)\mu^\beta(E_0)}\int_0^\infty r^{-\beta-1}\mathbb{P}\left(\mathcal{N}^{(r)}(A_1)\ \mathrm{odd}, \mathcal{N}^{(r)}(A_2)\ \mathrm{odd}\right)dr.\end{aligned} \tag{2.6}$$

We first compute the probability in the integrand. By discussing the even/odd cardinalities of $A_1\backslash A_2, A_2\backslash A_1, A_1\cap A_2$, we see that it is the same as

$$\begin{aligned}&\mathbb{P}\left(\mathcal{N}^{(r)}(A_1)\ \mathrm{odd}, \mathcal{N}^{(r)}(A_2)\ \mathrm{odd}\right)\\ &\qquad = \frac{1}{2}\left[\mathbb{P}\left(\mathcal{N}^{(r)}(A_1)\ \mathrm{odd}\right) + \mathbb{P}\left(\mathcal{N}^{(r)}(A_2)\ \mathrm{odd}\right) - \mathbb{P}\left(\mathcal{N}^{(r)}(A_1\Delta A_2)\ \mathrm{odd}\right)\right].\end{aligned}$$

So (2.6) becomes

$$\frac{\beta}{\Gamma(1-\beta)\mu^\beta(E_0)}\int_0^\infty \frac{r^{-\beta-1}}{4}\left(1-e^{-2\mu(A_1)r}+1-e^{-2\mu(A_2)r}-1+e^{-2\mu(A_1\Delta A_2)r}\right)dr.$$

With $\int_0^\infty \beta r^{-\beta-1}(1-e^{-ar})dr = a^\beta\Gamma(1-\beta)$ for $a>0$, the above becomes then

$$\begin{aligned}&\mathbb{P}\left(|R_\beta\cap A_1|\ \mathrm{odd}, |R_\beta\cap A_2|\ \mathrm{odd}\right)\\ &\qquad = \frac{1}{2^{1-\beta}\mu^\beta(E_0)}\cdot\frac{1}{2}\left(\mu^\beta(A_1)+\mu^\beta(A_2)-\mu^\beta(A_1\Delta A_2)\right).\end{aligned} \tag{2.7}$$

We now see that $Y_{2,\beta}$ and $\mathbb{B}_\mu^{\beta/2}$ share the same covariance function. This completes the proof. □

When restricted to $\alpha\in(0,2)$ the Karlin random field with representation (2.2) has the following series representation (see Samorodnitsky and Taqqu, 1994, Theorem 3.10.1),

$$\left\{Y_{\alpha,\beta}(A)\right\}_{A\in\mathcal{A}_0} \stackrel{d}{=} \left\{\sum_{j\in\mathbb{N}}\eta_{\alpha,j}\mathbf{1}_{\{|R_{\beta,j}\cap A|\ \mathrm{odd}\}}\right\}_{A\in\mathcal{A}_0}, \tag{2.8}$$

where $\{\eta_{\alpha,j}\}_{j\in\mathbb{N}}$ are enumerations of a Poisson point process on $\overline{\mathbb{R}}\backslash\{0\}$ with intensity

$$2^{1-\beta}\mu^\beta(E_0)\cdot\frac{\alpha C_\alpha}{2}|x|^{-\alpha-1}, x\neq 0,$$

with

$$C_\alpha := \left(\int_0^\infty x^{-\alpha-1}\sin x dx\right)^{-1}, \alpha\in(0,2),$$

and $\{R_{\beta,j}\}_{j\in\mathbb{N}}$ are i.i.d. copies of R_β, independent from $\{\eta_{\alpha,j}\}_{j\in\mathbb{N}}$.

2.2. *A general simulation framework.* The framework of Asmussen and Rosiński (2001) applies to $\{Y_{\alpha,\beta}(A)\}_{A\in\mathcal{A}_0}$ as follows. Take the random series on the right-hand side of (2.8) as the definition of $Y_{\alpha,\beta}(A)$. Then given $\epsilon > 0$, we write

$$Y_{\alpha,\beta}(A) = Y^{\epsilon,1}_{\alpha,\beta}(A) + Y^{\epsilon,2}_{\alpha,\beta}(A)$$

as the sum of the large-jump and the small-jump parts of the original process given by

$$\begin{aligned} Y^{\epsilon,1}_{\alpha,\beta}(A) &:= \sum_{j\in\mathbb{N}} \eta_{\alpha,j} \mathbf{1}_{\{|R_{\beta,j}\cap A| \text{ odd}\}} \mathbf{1}_{\{\eta_{\alpha,j}>\epsilon\}}, \\ Y^{\epsilon,2}_{\alpha,\beta}(A) &:= \sum_{j\in\mathbb{N}} \eta_{\alpha,j} \mathbf{1}_{\{|R_{\beta,j}\cap A| \text{ odd}\}} \mathbf{1}_{\{\eta_{\alpha,j}\leqslant\epsilon\}}, A \in \mathcal{A}_0, \end{aligned}$$

respectively. The large-jump part has a compound-Poisson representation

$$\left\{Y^{\epsilon,1}_{\alpha,\beta}(A)\right\}_{A\in\mathcal{A}_0} \stackrel{d}{=} \left\{\sum_{j=1}^{N_{\alpha,\epsilon}} V_{\alpha,\epsilon,j} D_{j,A}\right\}_{A\in\mathcal{A}_0} \quad \text{with } D_{j,A} := \mathbf{1}_{\{|R_{\beta,j}\cap A| \text{ odd}\}}, A \in \mathcal{A}_0, \tag{2.9}$$

where $N_{\alpha,\epsilon}$ is a Poisson random variable with parameter $2^{1-\beta}\mu^\beta(E_0)C_\alpha\epsilon^{-\alpha}$ and $\{V_{\alpha,\epsilon,j}\}_{j\in\mathbb{N}}$ are i.i.d. symmetric random variables with probability density function $\epsilon^\alpha(\alpha/2)|y|^{-\alpha-1}\mathbf{1}_{\{|y|>\epsilon\}}$, $\{R_{\beta,j}\}_{j\in\mathbb{N}}$ are i.i.d. copies of R_β, and all random variables are independent.

For the small-jump part, one can show the following.

Proposition 2.5. *With the notations above,*

$$\left\{\frac{Y^{\epsilon,2}_{\alpha,\beta}(A)}{\sigma_\alpha(\epsilon)}\right\}_{A\in\mathcal{A}_0} \stackrel{f.d.d.}{\Rightarrow} \left\{\mathbb{B}^{\beta/2}_\mu(A)\right\}_{A\in\mathcal{A}_0},$$

as $\epsilon \downarrow 0$, where $\{\mathbb{B}^{\beta/2}_\mu(A)\}_{A\in\mathcal{A}_0}$ is the set-indexed fractional Brownian motion with the covariance function (2.5).

Proof: The result follows from Proposition A.2 and Lemma 2.3. □

Now we look into implementation issues. For our examples, we always identify a set of indices T (a subset of $\mathbb{R}^d$ or $\mathbb{S}^d$) to $\{A_t\}_{t\in T} \subset \mathcal{A}_0$, and write simply from now on

$$\{Y_{\alpha,\beta}(t)\}_{t\in T} \equiv \{Y_{\alpha,\beta}(A_t)\}_{t\in T},$$

and similarly for the large-jump and small-jump parts. Now the above discussions suggest that the approximated process (in distribution) in simulation is

$$Y_{\alpha,\beta}(t) \approx Y^{\epsilon,1}_{\alpha,\beta}(t) + \sigma_\alpha(\epsilon)\mathbb{B}^{\beta/2}_\mu(t), t \in T. \tag{2.10}$$

While the large-jump part is compound Poisson and the approximated small-jump part is Gaussian, and both classes of stochastic processes in principle have exact simulation methods, computational issues arise quickly if one examines more closely.

For the large-jump part, clearly it suffices to sample the *odd-occupancy vector*

$$\boldsymbol{D} = (D_{t_1}, \ldots, D_{t_n}) \quad \text{with} \quad D_t := \mathbf{1}_{\{|R_\beta\cap A_t| \text{ odd}\}},$$

with a finite index lattice $T = \{t_1, \ldots, t_n\}$ in practice. A straightforward algorithm is the following.

Algorithm 2.6.

(1) Generate a β-Sibuya random variable Q_β.
(2) Sample $R_\beta \stackrel{d}{=} \bigcup_{i=1}^{Q_\beta}\{U_i\}$.
(3) Compute $\{D_t\}_{t\in T}$ based on the sampling of R_β.

In order to sample Q_β here, we recall a nice expression due to Sibuya (1979). Namely, with G_1, G_β and $G_{1-\beta}$ being three independent standard Gamma random variables with parameters 1, β and $1-\beta$, respectively, we have

$$Q_\beta \stackrel{d}{=} 1 + \mathrm{Poisson}\left(\frac{G_1 G_{1-\beta}}{G_\beta}\right), \tag{2.11}$$

where the second term on the right-hand side is understood as a Poisson random variable with a random parameter. So in practice we could first sample the random parameter $\Lambda = G_1G_{1-\beta}/G_\beta$ and then a Poisson random variable with parameter Λ, and add one to the sampled value at the end.

However, one should realize quickly that this algorithm is not computationally efficient, as the β-Sibuya distribution does not have finite β-th moment (e.g. Pitman, 2006). This could become quite cumbersome in practice as from time to time Q_β may be hundreds of thousands, while the resolution n in T_n is at most a few hundreds. It turns out that for Karlin stable processes and multiparameter fractional stable processes, one can exploit further the structure of $\mathcal{A}_0$ and sample $\boldsymbol{D}$ directly and much more efficiently, without sampling Q_β.

Remark 2.7. In practice one should decide also what value of ϵ makes a good approximation in (2.10). One may choose the value according to the Berry–Esseen bound on the Gaussian approximation (see Remark A.4), which for the marginal distribution in this case becomes (taking $(S,m) = (\Omega', 2^{1-\beta}\mu^\beta(E_0)\cdot\mathbb{P}')$ and $f_t(\omega') = D_t(\omega') = \mathbf{1}_{\{|R'_\beta(\omega')\cap A_t| \text{ odd}\}}$ as such that with respect to $\mathbb{P}'$ D'_t is a copy of D_t before)

$$C_{\mathrm{BE}}\frac{1}{(2^{1-\beta}\mu^\beta(E_0)\mathbb{E}D_t)^{1/2}}\frac{(2-\alpha)^{3/2}}{(3-\alpha)\sqrt{\alpha C_\alpha}}\epsilon^{\alpha/2} = C_{\mathrm{BE}}\frac{1}{\mu^{\beta/2}(A_t)}\frac{(2-\alpha)^{3/2}}{(3-\alpha)\sqrt{\alpha C_\alpha}}\epsilon^{\alpha/2},$$

where we used

$$\mathbb{E}D_t = \mathbb{P}(R_\beta\cap A_t \text{ odd}) = \mathbb{E}\left(\frac{1}{2}\left[1-\left(1-2\frac{\mu(A_t)}{\mu(E_0)}\right)^{Q_\beta}\right]\right) = 2^{\beta-1}\frac{\mu^\beta(A_t)}{\mu^\beta(E_0)}. \tag{2.12}$$

In Figure 2.2, the values of $\epsilon=\epsilon_\alpha$ such that

$$\frac{(2-\alpha)^{3/2}}{(3-\alpha)\sqrt{\alpha C_\alpha}}\epsilon^{\alpha/2} = 0.01$$

is plotted, along with C_α, $\sigma_\epsilon(\alpha)$ and $n_{\alpha,\epsilon} := C_\alpha\epsilon^{-\alpha}$, for $\alpha\in(0,2)$. Note that $n_{\alpha,\epsilon} = \mathbb{E}N_{\alpha,\epsilon}/(2^{1-\beta}\mu^\beta(E_0))$ and tells roughly (the terms depending on β is dropped for simple comparison) how many independent copies are needed for the large-jump part (2.9).

From the plot we see that, first, the small-jump part is far from negligible for α close to 2. Second, for $\alpha<1$ the gain of approximating small-jump part is very limited, while the cost of simulating the large-jump part is huge. This is not surprising as it is well known that when $\alpha<1$ the series representation is absolutely summable, and the magnitudes of small jumps decay as $O(j^{-1/\alpha})$. Therefore, in practice we choose not to apply the small-jump approximation for $\alpha<1$. See examples in Figure 1.1 for $\alpha=0.5$, where we set $\epsilon=10^{-4}$.

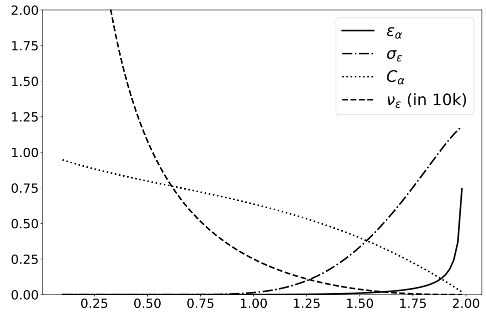

FIGURE 2.2. Comparison of parameters.

Remark 2.8. Another numerical issue that we encountered in implementing Algorithm 2.6 is that, due to the fact that $\Lambda = G_1 G_{1-\beta}/G_\beta$ is heavy-tailed, occasionally sampling Λ returns a very huge number that forbids the computation to continue (e.g. in Python on a 64-bit platform, an integer value is no bigger than $2^{63}-1$; the parameter of Poisson of Λ can easily go beyond this order during say 1000 i.i.d. sampling when $\beta < 0.2$). One way to go around this issue is to set up a threshold, say λ_0, and use Poisson$(\Lambda \wedge \lambda_0)$ instead of Poisson(Λ) in Algorithm 2.6. Then, the probability that the threshold is exceeded at least once (and hence the simulation is only an approximation) is bounded by $\mathbb{P}(\bigcup_{i=1}^{N_{\alpha,\epsilon}}\{\Lambda_i > \lambda_0\}) \leqslant \mathbb{E}N_{\alpha,\epsilon}\mathbb{P}(\Lambda > \lambda_0)$.

For the small-jump part, the by-default method of applying the Cholesky decomposition to a covariance matrix of size $n \times n$ is computationally infeasible for high dimensions (with complexity $O(n^3)$, and $\mathbb{R}^2$- or $\mathbb{S}^2$-indexed processes a reasonable resolution requires n to be at least 200^2). In a few cases, we are in a fortunate situation that the set-indexed fractional Brownian motion is known to have a fast and exact simulation method. The only exception is the case when it is a multi-parameter fractional Brownian motion, for which we develop a fast approximation method. The simulation methods are summarized in Table 2.1.

In the next section we provide details for simulations for a few examples. Table 2.1 is a summary on where improvement can be made regarding simulation efficiency.

3. Examples

Recall that we work with Karlin random fields $\{Y_{\alpha,\beta}(A_t)\}_{t\in T}$ in (2.8), with a measure space $(E, \mathcal{E}, \mu)$, $E_0 \in \mathcal{E}$ with $\mu(E_0) < \infty$, and an index set $\{A_t\}_{t\in T}$ such that $A_t \subset E_0$. The four examples summarized in Table 2.1 are worked out below one by one.

3.1. *Karlin stable processes.* This example corresponds to the choice of

$$(E, \mathcal{E}, \mu) \equiv (\mathbb{R}_+, \mathcal{B}(\mathbb{R}_+), \mathrm{Leb}), E_0 = [0,1], \text{ and } \{A_t\}_{t\in[0,1]} = \{[0,t]\}_{t\in[0,1]}.$$

Table 2.1. Summary of simulation methods for examples in Section 3. The column 'E' indicates the underlying space $(E, \mathcal{E})$. The column '$\boldsymbol{D}$' indicates whether the odd-occupancy vector can be sampled in an efficient way without sampling the entire R_β. The last column indicates the set-indexed fractional Brownian motion that approximates the small-jump part, and the corresponding simulation method. Acronyms used below are, fLCsf: fractional Lévy–Chenstov stable field; mfsf: multiparameter fractional stable field; (m/s)fBm: (multiparameter/spherical) fractional Brownian motion, fLBf: fractional Lévy–Brownian field, CEM: circulant embedding method; IEM: intrinsic embedding method.

Sec.	Example	E	$\boldsymbol{D}$	set-indexed fBm
3.1	Karlin ($\mathbb{R}_+$-indexed fLCsf)	$\mathbb{R}_+$	fast	fBm, CEM (Wood and Chan, 1994 Dietrich and Newsam, 1997)
3.2	mfsf	$\mathbb{R}_+^2$	fast	mfBm, Prop. 3.5
3.3	$\mathbb{R}^2$-indexed fLCsf	$\mathbb{S} \times \mathbb{R}_+$	slow	fLB, IEM (Stein, 2002)
3.4	$\mathbb{S}^2$-indexed fLCsf	$\mathbb{S}^2$	slow	sfBm, CEM (Cuevas et al., 2020)

The large-jump part. In this case, we introduce an algorithm that improves significantly the efficiency of Algorithm 2.6 when simulating the odd-occupancy vectors, thanks to the structure of $\{A_t\}_{t\in[0,1]}$. Note that in simulation we only need to work with an index set $T = \{t_1, \dots, t_n\}$ with $0 \leqslant t_1 < \cdots < t_n \leqslant 1$. Let N_{Λ_β} be a Poisson random variable with a random parameter $\Lambda_\beta := G_1 G_{1-\beta}/G_\beta$, where G_1, G_β and $G_{1-\beta}$ are as in (2.11). We introduce this time

$$\widetilde{R}_\beta := \bigcup_{i=1}^{N_{\Lambda_\beta}} \{U_i\},$$

where $\{U_i\}_{i\in\mathbb{N}}$ are i.i.d. uniform random variables over $(0, 1)$ independent from N_{Λ_β}. Let U be another uniform random variable independent from $\{U_i\}_{i\in\mathbb{N}}$. Define

$$M_i := \sum_{j=1}^{i} B_j + \mathbf{1}_{\{U\in(0,t_i]\}} \quad \text{with} \quad B_i := \mathbf{1}_{\left\{\left|\widetilde{R}_\beta\cap(t_{i-1},t_i]\right| \text{ odd}\right\}}, i = 1, \dots, n. \tag{3.1}$$

Then, the Sibuya identity (2.11) says that $N_{\Lambda_\beta} + 1 \stackrel{d}{=} Q_\beta$, and hence

$$\{D_{t_i}\}_{i=1,\dots,n} \stackrel{d}{=} \{M_i \bmod 2\}_{i=1,\dots,n}. \tag{3.2}$$

The advantage of this representation is that the random vector $\boldsymbol{M} = (M_1, \dots, M_n)$, or essentially $\boldsymbol{B} = (B_1, \dots, B_n)$, can be simulated as a collection of conditionally independent Bernoulli random variables, and hence with linear complexity in n *without sampling the heavy-tailed* N_{Λ_β} (see Remark 3.3 below), thanks to the following simple fact.

Lemma 3.1. *With the notations above, given Λ_β, $\{B_i\}_{i=1,\dots,n}$ are conditionally independent Bernoulli random variables with parameters*

$$p_i(\Lambda_\beta) = \frac{1}{2}\left(1 - e^{-2(t_i - t_{i-1})\Lambda_\beta}\right), i = 1, \dots, n. \tag{3.3}$$

Proof: Given Λ_β, $\widetilde{R}_\beta$ is the collection of all points of a Poisson point process on $(0,1)$ with intensity Λ_β. Then by independent scattering, we have that $\{B_i\}_{i=1,\dots,n}$ are conditionally independent since $\{(t_{i-1},t_i]\}_{i=1,\dots,n}$ are disjoint. The corresponding parameter of each follows from the fact that, for a Poisson random variable Z with parameter $\lambda > 0$, $\mathbb{P}(Z \text{ odd}) = (1-\mathrm{e}^{-2\lambda})/2$. □

Below is a summary of our improved algorithm for simulating $\boldsymbol{D}$.

Algorithm 3.2.

(1) Sample $\Lambda_\beta \overset{d}{=} G_1 G_{1-\beta}/G_\beta$.
(2) Given Λ_β, sample independent $B_i \sim \mathrm{Ber}(p_i(\Lambda_\beta)), i=1,\dots,n$ (3.3).
(3) Sample $U \sim \mathrm{Unif}(0,1)$.
(4) Compute $\boldsymbol{M}$ as in (3.1) and $\boldsymbol{D} = \boldsymbol{M} \bmod 2$ as in (3.2).

Remark 3.3. Algorithm 2.6 requires Q_β number of exact locations of i.i.d. random variables $\{U_i\}_{i\in\mathbb{N}}$, and this shall be repeated $N_{\alpha,\epsilon}$ times. The random variable $N_{\alpha,\epsilon}$ is Poisson and hence well concentrated at its mean $2^{1-\beta}\mu^\beta(E_0)C_\alpha\epsilon^{-\alpha}$. Viewing $N_{\alpha,\epsilon}$ as a fixed number for comparison, we see that this requires $\sum_{i=1}^{N_{\alpha,\epsilon}} Q_{\beta,i}\cdot n$ number of iterations to sample the large-jump part, with $\{Q_{\beta,i}\}_{i\in\mathbb{N}}$ being i.i.d. copies of Q_β. By the central limit theorem, we know that $N_{\alpha,\epsilon}^{-1/\beta}\sum_{i=1}^{N_{\alpha,\epsilon}} Q_{\beta,i}$ has, for $\epsilon > 0$ very small, approximately the totally skewed β-stable distribution (without finite β-th moment), say Z_β. So roughly Algorithm 2.6 has a complexity of order $Z_\beta \cdot N_{\alpha,\epsilon}^{1/\beta}\cdot n$. On the other hand, Algorithm 3.2 has a complexity of order $N_{\alpha,\epsilon}\cdot n$, which is much lower.

The small-jump part. In this case, simulating the small-jump part is straightforward, as the set-indexed fractional Brownian motion is $\{\mathbb{B}_\mu^{\beta/2}([0,t])\}_{t\geqslant 0} \equiv \{\mathbb{B}^{\beta/2}(t)\}_{t\geqslant 0}$ the fractional Brownian motion with Hurst index $\beta/2 \in (0,1/2)$ with covariance function as in (1.2). It is well known that fractional Brownian motions can be simulated in an exact and efficient manner by the circulant embedding method (e.g. Wood and Chan, 1994; Dietrich and Newsam, 1997; Perrin et al., 2002).

Simulations. In Figure 3.3, we provide a few simulation results for the odd-occupancy vector. In Figure 3.4, we provide a few simulation results for the Karlin stable processes. The simulations are over a lattice $\{i/n\}_{i=0,\dots,n}$ with $n=1000$.

3.2. *Multiparameter fractional stable fields.* In this case, we take

$$(E,\mathcal{E},\mu) = (\mathbb{R}_+^2, \mathcal{B}(\mathbb{R}_+^2), \mathrm{Leb}), E_0 = [\boldsymbol{0},\boldsymbol{1}], \text{ and } \{A_{\boldsymbol{t}}\}_{\boldsymbol{t}\in[\boldsymbol{0},\boldsymbol{1}]} = \{[\boldsymbol{0},\boldsymbol{t}]\}_{\boldsymbol{t}\in[\boldsymbol{0},\boldsymbol{1}]}. \quad (3.4)$$

(In this section, $[\boldsymbol{a},\boldsymbol{b}] = [a_1,b_1]\times[a_2,b_2]$ for $\boldsymbol{a}=(a_1,a_2), \boldsymbol{b}=(b_1,b_2)\in\mathbb{R}_+^2$.)

The large-jump part. Again, $\{A_{\boldsymbol{t}}\}_{\boldsymbol{t}\in[\boldsymbol{0},\boldsymbol{1}]^2}$ has a nice structure that we can exploit to obtain an efficient algorithm for sampling $\boldsymbol{D}$ as in Algorithm 3.2. We only present a brief summary below as the proof is the same. This time the index lattice T is given by

$$T := \left\{\left(t_i^{(1)}, t_j^{(2)}\right) : t_i^{(r)} \in T^{(r)}, r=1,2\right\}, \text{ with } T^{(r)} := \left\{t_i^{(r)}\right\}_{i=1,\dots,n} \subset \mathbb{R}_+, r=1,2.$$

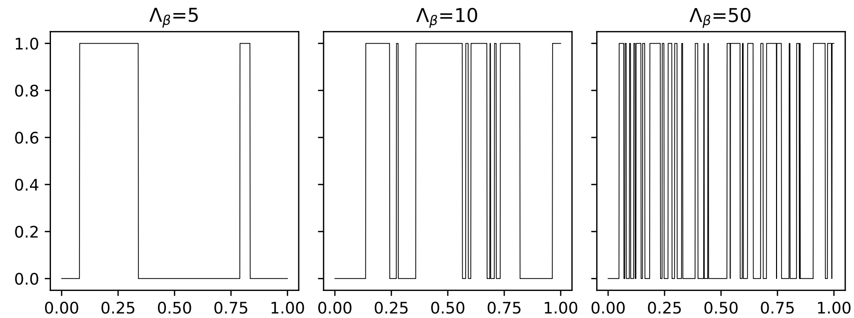

FIGURE 3.3. Simulations of odd-occupancy vectors with different Λ_β.

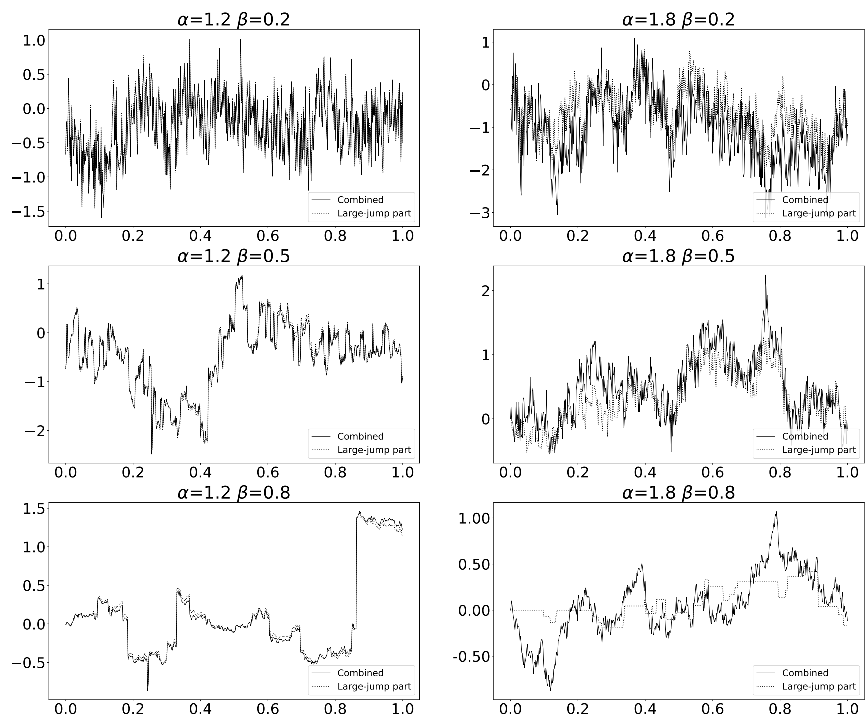

FIGURE 3.4. Simulations of Karlin stable processes.

Again we assume $t_i^{(r)}$ is increasing in i for $r = 1, 2$. This time we want to sample in law the vector $\boldsymbol{D} = \{D_{i,j}\}_{i,j=1,\dots,n}$ with

$$D_{i,j} \equiv D_{t_i^{(1)},t_j^{(2)}} := \mathbf{1}_{\left\{\left|R_\beta\cap[0,t_i^{(1)}]\times[0,t_j^{(2)}]\right|\text{ odd}\right\}}, i,j = 1,\dots,n.$$

Let Λ_β be as before (see (2.11)). This time introduce $\{B_{i,j}\}_{i,j=1,\dots,n}$ as conditionally independent Bernoulli random variables, given Λ_β, with parameters

$$p_{i,j}(\Lambda_\beta) = \frac{1}{2}\left(1 - e^{-2(t_i^{(1)}-t_{i-1}^{(1)})(t_j^{(2)}-t_{j-1}^{(2)})\Lambda_\beta}\right), i,j = 1,\dots,n, \tag{3.5}$$

with the convention $t_0^{(r)} = 0, r = 1, 2$. Let $\boldsymbol{U}$ be another independent uniform random vector in $(\mathbf{0}, \mathbf{1})$. Then, with

$$M_{i,j} := \sum_{k=1}^{i}\sum_{\ell=1}^{j} B_{k,\ell} + \mathbf{1}_{\left\{\boldsymbol{U}\in(0,t_i^{(1)}]\times(0,t_j^{(2)}]\right\}}, i, j = 1, \dots, n, \tag{3.6}$$

by the same argument as in Lemma 3.1 we have that

$$\{D_{i,j}\}_{i,j=1,\dots,n} \stackrel{d}{=} \{M_{i,j} \bmod 2\}_{i,j=1,\dots,n} \,. \tag{3.7}$$

In summary, we use the following algorithm to sample the odd-occupancy vector $\boldsymbol{D}$ of the multiparameter fractional stable fields.

Algorithm 3.4.

(1) Sample $\Lambda_\beta \stackrel{d}{=} G_1 G_{1-\beta}/G_\beta$.
(2) Given Λ_β, sample independent $B_{i,j} \sim \mathrm{Ber}(p_{i,j}(\Lambda_\beta)), i, j = 1, \dots, n$ (3.5).
(3) Sample $\boldsymbol{U} \sim \mathrm{Unif}(\mathbf{0}, \mathbf{1})$.
(4) Compute $\boldsymbol{M}$ as in (3.6) and $\boldsymbol{D} = \boldsymbol{M}$ as in (3.7).

The small-jump part. It turns out that the set-indexed process $\{\mathbb{B}_\mu^{\beta/2}([\mathbf{0}, \boldsymbol{t}])\}_{\boldsymbol{t}\in\mathbb{R}_+^2} \equiv \{\mathbb{B}^{\beta/2}(\boldsymbol{t})\}_{\boldsymbol{t}\geqslant 0}$ becomes the multiparameter fractional Brownian motion (Herbin and Merzbach, 2007) with covariance function (1.3). This random field does not have stationary increments, and we are not aware of any exact sampling method that works efficiently with this covariance function. Instead, we propose to apply the following aggregation approximation for simulating the small-jump part. The general idea of aggregation approximation is, instead of applying the deterministic Cholesky decomposition of the given covariance matrix Σ, to find an easy-to-simulate random vector ($\boldsymbol{D}$ here) so that $\Sigma = \mathbb{E}(\boldsymbol{D}'^t\boldsymbol{D})$ (here $\boldsymbol{D}'^t$ is the transpose of $\boldsymbol{D}'$, an independent copy of $\boldsymbol{D}$). Below, recall that in this section we identify $\mathcal{A}_0 = \{A_{\boldsymbol{t}}\}_{\boldsymbol{t}\in[\mathbf{0},\mathbf{1}]}$. We also keep the factor $\mu(E_0)$ below, although for set-indexed fractional Brownian motion (3.4), $\mu(E_0) = 1$.

Proposition 3.5. *Let $\{\varepsilon_j\}_{j\in\mathbb{N}}$ be a sequence of i.i.d. standard normal random variables and $\{\boldsymbol{D}_j\}_{j\in\mathbb{N}}$ be i.i.d. copies as in (2.9). Then we have*

$$(2^{1-\beta}\mu^\beta(E_0))^{1/2} \cdot \left\{\frac{1}{\sqrt{m}}\sum_{j=1}^{m} \varepsilon_j D_{j,\boldsymbol{t}}\right\}_{\boldsymbol{t}\in[\mathbf{0},\mathbf{1}]} \stackrel{f.d.d.}{\Rightarrow} \left\{\mathbb{B}^{\beta/2}(\boldsymbol{t})\right\}_{\boldsymbol{t}\in[\mathbf{0},\mathbf{1}]}, \tag{3.8}$$

as $m \to \infty$, with $\mathbb{B}^{\beta/2}$ determined by (2.5).

Proof: By the multivariate central limit theorem, it suffices to compute to the asymptotic covariance of the left hand side of (3.8). That is, for $\boldsymbol{s}, \boldsymbol{t} \in [\mathbf{0}, \mathbf{1}]$,

$$\mathrm{Cov}(D_{\boldsymbol{s}}, D_{\boldsymbol{t}}) = \mathbb{E}(D_{\boldsymbol{s}} D_{\boldsymbol{t}}) = \mathbb{P}\left(|R_\beta \cap A_{\boldsymbol{s}}| \text{ odd}, |R_\beta \cap A_{\boldsymbol{t}}| \text{ odd}\right).$$

We have seen this computation in (2.7). □

Since $|D_{\boldsymbol{t}}| \leqslant 1$, we have a Berry–Esseen upper bound as $3.3/\sqrt{m}$ (Chen et al., 2011, Theorem 3.4). Applying the standard Berry–Esseen bound for the sum of i.i.d. centered random variables with unit variance (Korolev and Shevtsova, 2012), we have (recall (2.12))

$$C_{\rm BE}\frac{\mathbb{E}|D_{\boldsymbol t}|^3}{(\mathbb{E}|D_{\boldsymbol t}|^2)^{3/2}}m^{-1/2} = C_{\rm BE}\mathbb{P}(|R_\beta\cap A_{\boldsymbol t}|\ \mathrm{odd})^{-1/2}m^{-1/2}$$
$$= C_{\rm BE}\left(2^{\beta-1}\frac{\mu^\beta(A_t)}{\mu^\beta(E_0)}\right)^{-1/2}m^{-1/2}, \qquad (3.9)$$

as a Berry–Esseen upper bound for the convergence of (3.8).

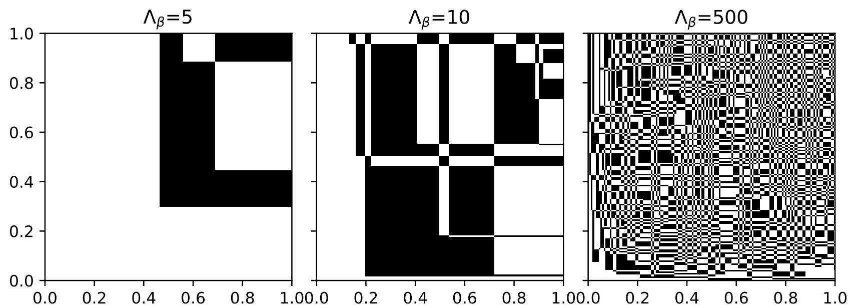

FIGURE 3.5. Simulations for odd-occupancy vectors for multiparameter stable fields with different values of Λ_β.

Simulations. Figure 3.5 provides a few simulations of the odd-occupancy vectors. Figure 3.6 provides a few simulations for the multiparameter fractional stable fields. The random field is sampled over a 300×300 lattice. For the small-jump part we take $m = 2500$ in Proposition 3.5 in view of the Berry–Esseen bound (3.9) (so that $m^{-1/2} = 2\%$).

3.3. *Fractional Lévy–Chentsov stable fields.* In this case, we take

$$(E,\mathcal{E},\mu) = \left(\mathbb{S}^1\times\mathbb{R}_+, \mathcal{B}(\mathbb{S}^1\times\mathbb{R}_+), d\boldsymbol{s}dr\right),$$

where $d\boldsymbol{s}dr$ is the product measure of the uniform measure $d\boldsymbol{s}$ on $\mathbb{S}^1$ and the Lebesgue measure dr on $\mathbb{R}_+$, and in practice we may restrict to

$$E_0 = \mathbb{S}^1\times[0,\sqrt{2}] \quad \text{and} \quad \{A_{\boldsymbol t}\}_{\boldsymbol{t}\in[\boldsymbol{0},\boldsymbol{1}]} = \left\{(\boldsymbol{s},r) : \boldsymbol{s}\in\mathbb{S}^1, 0<r<\langle\boldsymbol{s},\boldsymbol{t}\rangle\right\}_{\boldsymbol{t}\in[\boldsymbol{0},\boldsymbol{1}]},$$

with $\mu(E_0) = \sqrt{2}\cdot 2\pi$. (Actually, one could further restrict to $([0,\pi]\cup[3\pi/2,2\pi))\times[0,1]\subset E_0$ to gain some extra computational efficiency.) In this case, $\{\mathbb{B}_\mu^{\beta/2}(A_{\boldsymbol t})\}_{\boldsymbol{t}\in[\boldsymbol{0},\boldsymbol{1}]} \equiv \{\mathbb{B}^{\beta/2}(\boldsymbol{t})\}_{\boldsymbol{t}\in\in[\boldsymbol{0},\boldsymbol{1}]}$ becomes a fractional Lévy Brownian field, a centered Gaussian random field with covariance function (1.4).

The large-jump part. The nice lattice structure of $\{A_{\boldsymbol t}\}$ in the previous two examples is lost here, and it seems that we have to rely on Algorithm 2.6 to sample the large-jump part, which is computationally inefficient.

The small-jump part. It is well known that the intrinsic embedding method by Stein (2002) can be applied to simulate exactly and efficiently the fractional Lévy Brownian fields.

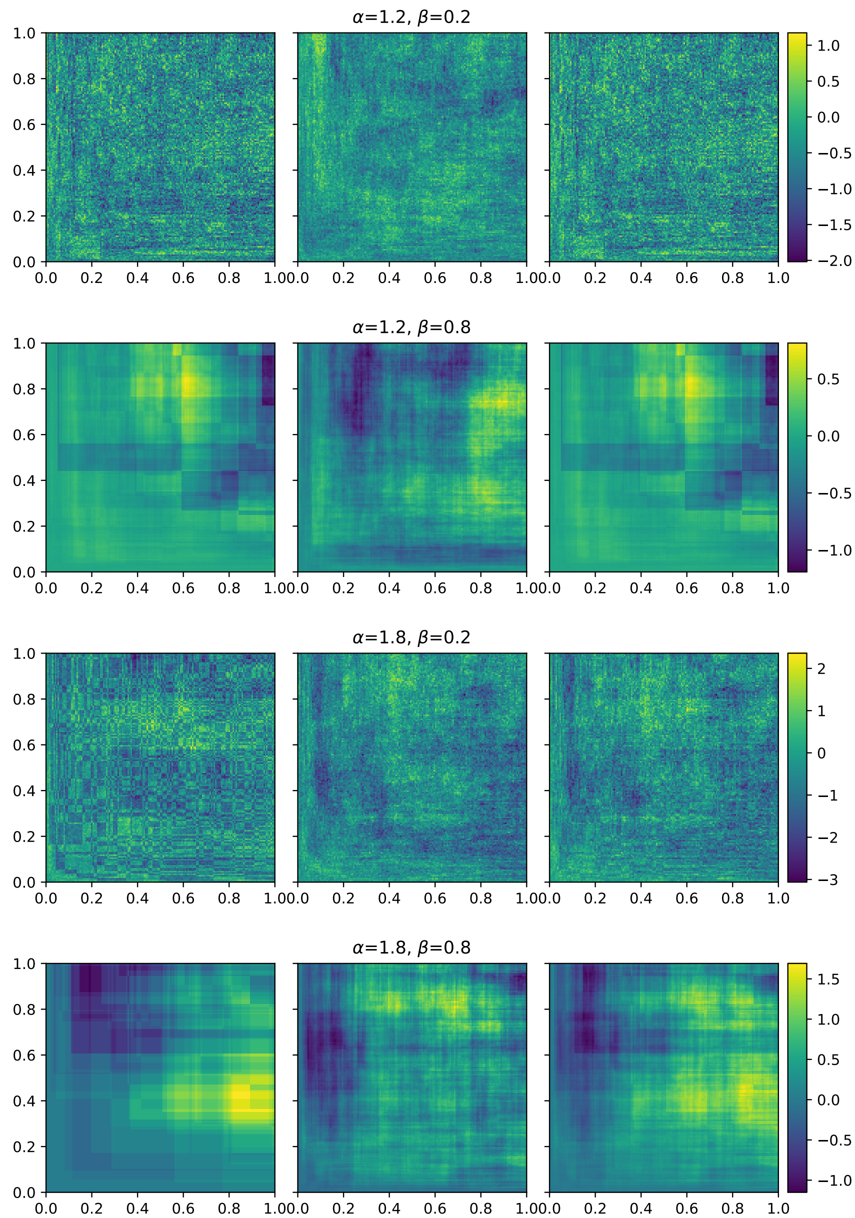

FIGURE 3.6. Simulations for multiparameter fractional stable fields. From left to right: the large-jump parts, the small-jump parts, and the combined fields.

Simulations. Figure 3.7 provides a few simulations for the odd-occupancy vectors for the fractional Lévy–Chentsov stable fields. Figure 3.8 provides a few simulations for the fractional Lévy–Chentsov stable fields. The random fields are sampled over a 300×300 lattice.

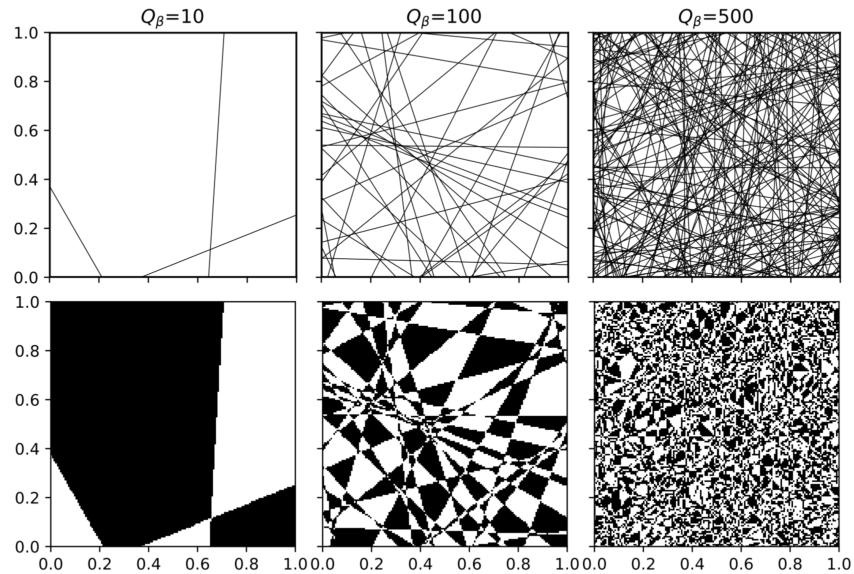

FIGURE 3.7. Simulations for odd-occupancy vectors for fractional Lévy–Chentsov stable fields with different Q_β. The plots in first row are i.i.d. Q_β hyperplanes (some may not intersect the region $[0,1]^2$), and the plots in the second row are the corresponding odd-occupancy vectors over a 300×300 lattice.

3.4. *Spherical fractional Lévy–Chenstov stable fields.* In this case, we take

$$(E, \mathcal{E}, \mu) = (\mathbb{S}^2, \mathcal{B}(\mathbb{S}^2), d\boldsymbol{s}), E_0 = E,$$

where $d\boldsymbol{s}$ is the Lebesgue measure on the unit sphere $\mathbb{S}^2$ in $\mathbb{R}^3$, and

$$A_{\boldsymbol{x}} = H_{\boldsymbol{x}} \triangle H_{\boldsymbol{o}}, \boldsymbol{x} \in \mathbb{S}^2 \quad \text{with} \quad H_{\boldsymbol{x}} := \left\{\boldsymbol{y} \in \mathbb{S}^2 : \langle \boldsymbol{x}, \boldsymbol{y} \rangle > 0\right\},$$

where $\boldsymbol{o} \in \mathbb{S}^2$ is the fixed north pole, and $H_{\boldsymbol{x}}$ is the hemisphere of $\mathbb{S}^2$ determined by $\boldsymbol{x}$. The spherical fractional Lévy–Chentsov stable field, denoted by $\{Y_{\alpha,\beta}(\boldsymbol{x})\}_{\boldsymbol{x}\in\mathbb{S}^2} \equiv \{Y_{\alpha,\beta}(A_{\boldsymbol{x}})\}_{\boldsymbol{t}\in\mathbb{S}^2}$, can be obtained by

$$\{Y_{\alpha,\beta}(\boldsymbol{x})\}_{\boldsymbol{x}\in\mathbb{S}^2} \stackrel{d}{=} \left\{\widetilde{Y}_{\alpha,\beta}(\boldsymbol{x}) - \widetilde{Y}_{\alpha,\beta}(\boldsymbol{o})\right\}_{\boldsymbol{x}\in\mathbb{S}^2}, \quad \text{with} \quad \widetilde{Y}_{\alpha,\beta}(\boldsymbol{x}) := \widetilde{Y}_{\alpha,\beta}(H_{\boldsymbol{x}}), \boldsymbol{x} \in \mathbb{S}^2. \tag{3.10}$$

The random field $\{\widetilde{Y}_{\alpha,\beta}(\boldsymbol{x})\}_{\boldsymbol{x}\in\mathbb{S}^2}$ is again a special case of Karlin random fields. In addition, it is rotationally stationary (a.k.a. strongly isotropic), and the discussions below are for $\widetilde{Y}_{\alpha,\beta}$ instead of $Y_{\alpha,\beta}$.

The large-jump part. We rely on Algorithm 2.6 to simulate the large-jump part.

The small-jump part. An advantage of working with $\widetilde{Y}_{\alpha,\beta}$ instead of $Y_{\alpha,\beta}$ is that now, Proposition 2.5 says that the small-jump part is approximated by a rotationally stationary spherical Gaussian field, denoted by $\{\widetilde{\mathbb{B}}^{\beta/2}(\boldsymbol{x})\}_{\boldsymbol{x}\in\mathbb{S}^2}$. Thanks to the rotational stationarity, such Gaussian random fields can be simulated fast and exactly by the circulant embedding method (Cuevas et al., 2020).

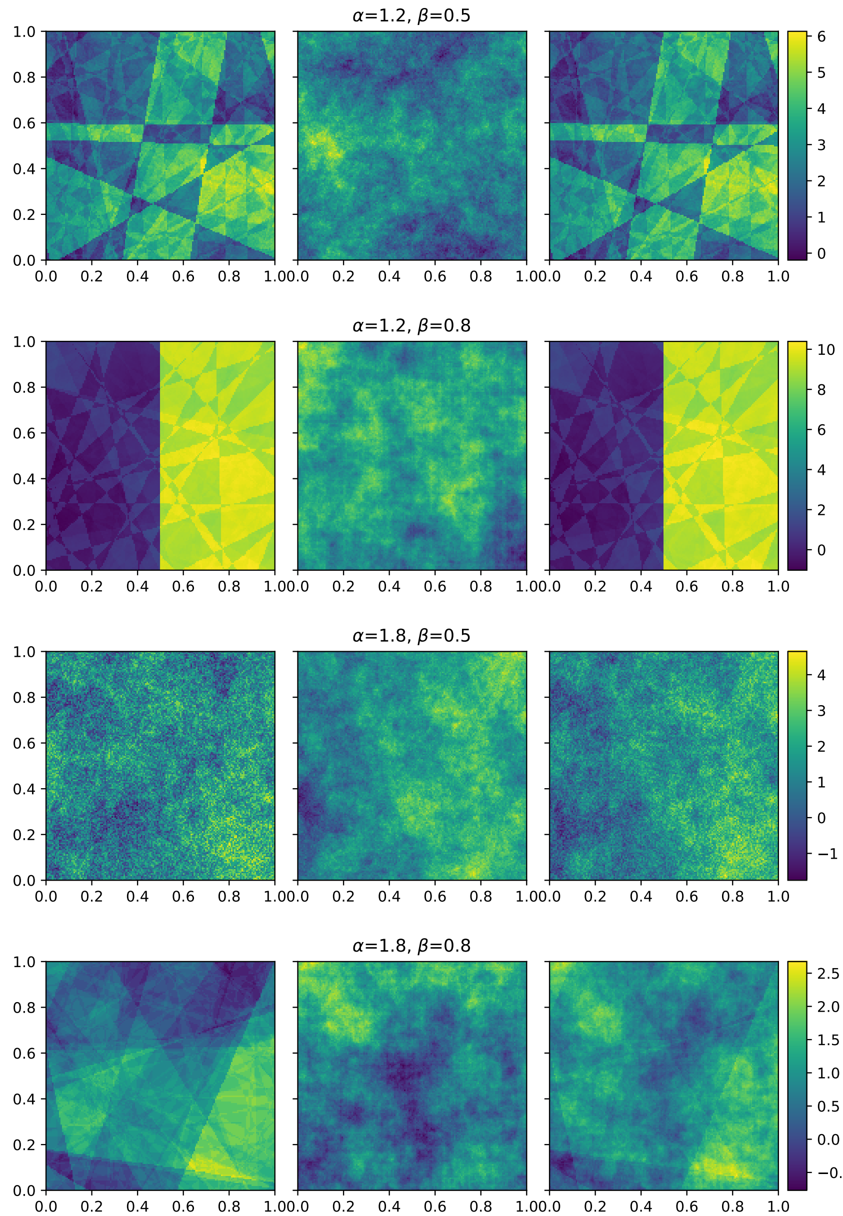

FIGURE 3.8. Simulations for fractional Lévy–Chentsov stable fields. From left to right: the large-jump parts, the small-jump parts, and the combined fields.

It remains to compute the covariance explicitly. In view of Proposition 2.5, $\widetilde{\mathbb{B}}^{\beta/2}$ is a set-indexed fractional Brownian motion with the same law as $Y_{2,2H}(H_{\boldsymbol{x}})$ (see (2.2)), where $H_{\boldsymbol{x}}$ is the hemisphere determined by $\boldsymbol{x} \in \mathbb{S}^2$ and μ the Lebesgue measure on $\mathbb{S}^2$ so that $\mu(H_{\boldsymbol{x}}) = 2\pi$ and $\mu(H_{\boldsymbol{x}}\Delta H_{\boldsymbol{y}}) = 4\mathsf{d}(\boldsymbol{x},\boldsymbol{y})$. Therefore, we have

$$\begin{aligned}\operatorname{Cov}\left(\widetilde{\mathbb{B}}^{\beta/2}(\boldsymbol{x}), \widetilde{\mathbb{B}}^{\beta/2}(\boldsymbol{y})\right) &= \operatorname{Cov}(Y_{2,2H}(H_{\boldsymbol{x}}), Y_{2,2H}(H_{\boldsymbol{y}}))\\ &= \frac{1}{2}\left(\mu^{2H}(H_{\boldsymbol{x}}) + \mu^{2H}(H_{\boldsymbol{y}}) - \mu^{2H}(H_{\boldsymbol{x}}\Delta H_{\boldsymbol{y}})\right)\\ &= (2\pi)^{2H}\left(1 - \frac{1}{2}\left(\frac{2}{\pi}\right)^{2H}\mathsf{d}^{2H}(\boldsymbol{x},\boldsymbol{y})\right).\end{aligned}$$

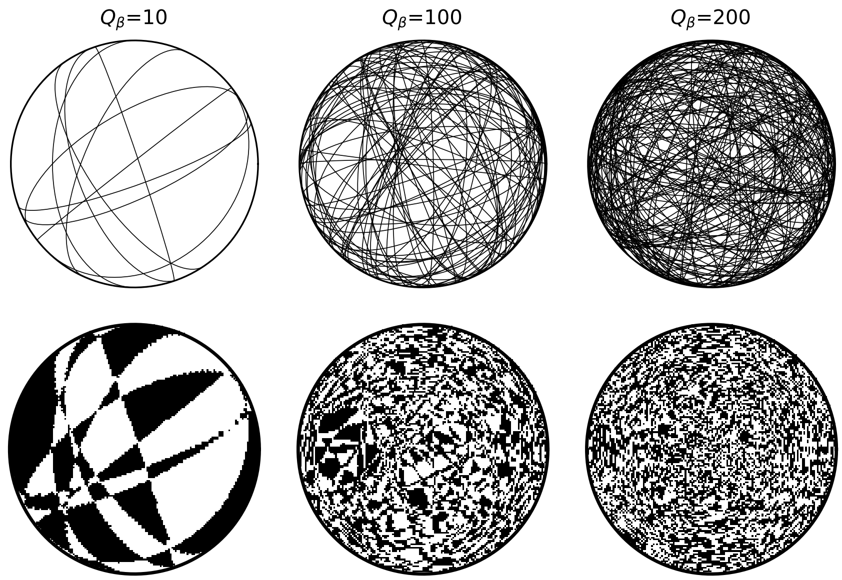

FIGURE 3.9. Simulations for odd-occupancy vectors for spherical fractional Lévy–Chentsov stable fields for different Q_β. The plots in first row are the great circles corresponding to i.i.d. Q_β points from the sphere, and the plots in the second row are the corresponding odd-occupancy vectors over a 300×150 lattice in polar coordinates.

Simulations. Figure 3.9 provides a few simulations for the odd-occupancy vectors for spherical fractional Lévy–Chentsov fields. Figure 3.10 provides a few simulations for the spherical fractional Lévy–Chentsov fields. The spherical random fields are sampled over a 300×150 lattice in the polar coordinates. For simulation examples of $Y_{\alpha,\beta}$, see Figure 1.1, where we sampled the approximated $\widetilde{Y}_{\alpha,\beta}$ first and applied the pinning-down relation (3.10).

Acknowledgement. The authors would like to thank an anonymous referee for very helpful and constructive comments. YW would like to thank Yimin Xiao for helpful discussions on spherical fractional Brownian motions. ZF and YW's research were partially supported by Army Research Office grant W911NF-17-1-0006.

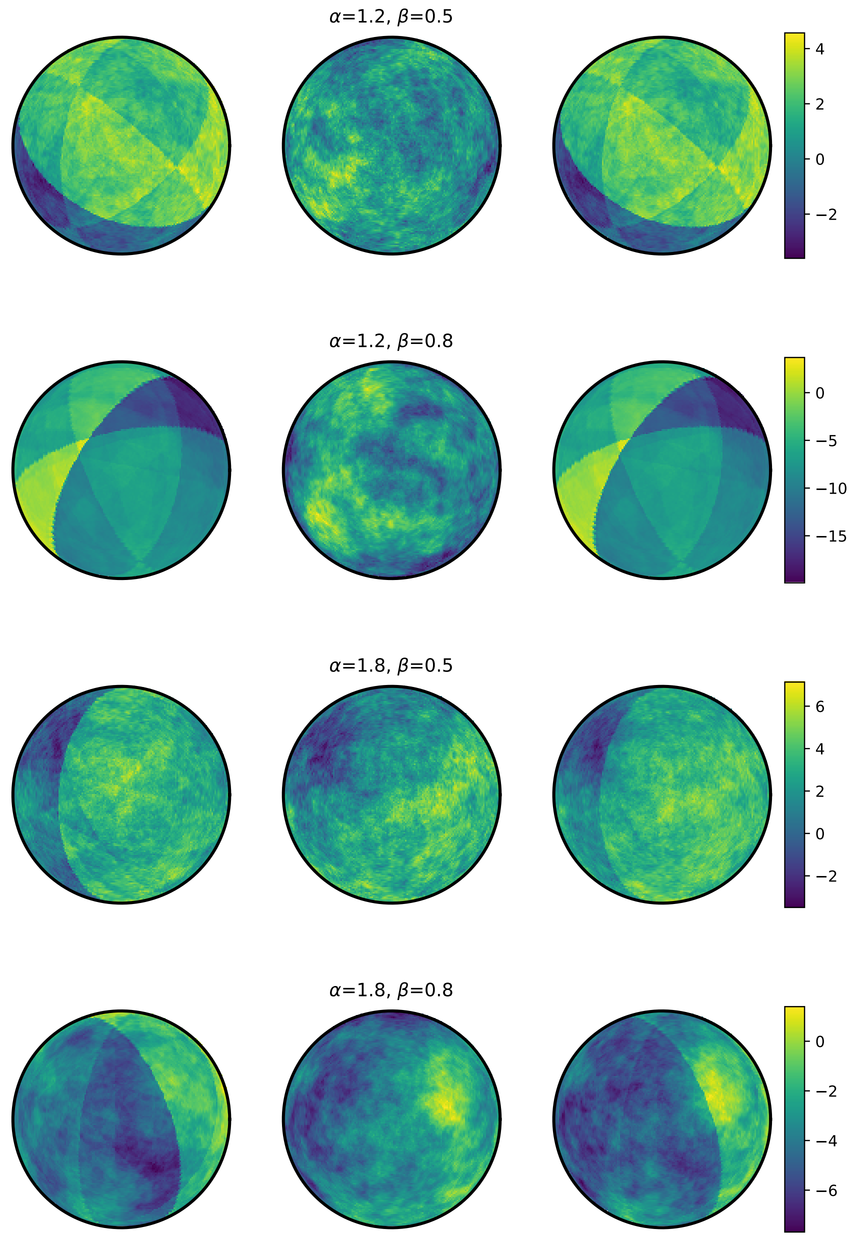

FIGURE 3.10. Simulations for rotationally stationary spherical fractional Lévy–Chentsov stable fields. From left to right: the large-jump parts, the small-jump parts, and the combined fields.

Appendix A. A general framework for simulating stable processes

The framework here can be read from Cohen et al. (2008) where an essentially more general one for infinitely-divisible processes is explained in details. We only focus on a subclass of $S\alpha$S processes, of which the task is significantly simplified (see Remark A.3). Namely, for some measurable space $(S, \mathcal{S})$ equipped with a *finite measure* m and a family of *square integrable functions* $\{f_t\}_{t\in T}$ on (S, m), we are interested in simulating SαS processes defined as

$$X(t) := \sum_{j\in\mathbb{N}} \eta_{\alpha,j} f_t(W_j), t \in T, \alpha \in (0,2), \tag{A.1}$$

where

$$\{(\eta_{\alpha,j}, W_j)\}_{j\in\mathbb{N}} \sim \text{PPP}\left(\frac{\alpha C_\alpha}{2}|y|^{-\alpha-1}dydm\right).$$

Remark A.1. Alternatively, the above can be viewed as a Poisson point process with i.i.d. marks, with $\{\eta_{\alpha,j}\}_{j\in\mathbb{N}} \sim \text{PPP}((1/2)C_\alpha m(S)\alpha|y|^{-\alpha-1}dy)$ on $\overline{\mathbb{R}}\backslash\{0\}$ and $\{W_j\}_{j\in\mathbb{N}}$ as i.i.d. random elements in S with law $m(\cdot)/m(S)$, two families being independent. This representation is helpful for some analysis of the stable processes, but is not needed in our proofs.

The definition (A.1) has the following stochastic-integral representation

$$\{X(t)\}_{t\in T} \stackrel{d}{=} \left\{\int_S f_t(s) M_\alpha(ds)\right\}_{t\in T}, \alpha \in (0,2), \tag{A.2}$$

where M_α is an SαS random measure on $(S, \mathcal{S})$ with control measure m (Samorodnitsky and Taqqu, 1994, Corollary 3.10.4). In general, the representations of stable processes, in particular the choices of (S, m), are not unique, and a good choice may increase significantly the efficiency of simulation method.

It is well known that, when $\alpha \in (0,2)$, there are no exact simulation methods for most SαS processes. In the seminal work of Asmussen and Rosiński (2001), it was pointed out that in simulations, the SαS process should be decomposed into the large-jump and small-jump parts, and then the two parts could be simulated independently. Namely, let $\epsilon > 0$, in view of (A.1), the process $\{X(t)\}_{t\in T}$ can be written as the sum of two independent processes

$$X(t) = X_{\epsilon,1}(t) + X_{\epsilon,2}(t),$$

with $X_{\epsilon,1}$ and $X_{\epsilon,2}$ given by

$$X_{\epsilon,1}(t) := \sum_{n=1}^{\infty} \eta_{\alpha,n} f_t(W_n) \mathbf{1}_{\{\eta_{\alpha,n} \geqslant \epsilon\}}, \text{ and } X_{\epsilon,2}(t) := \sum_{n=1}^{\infty} \eta_{\alpha,n} f_t(W_n) \mathbf{1}_{\{\eta_{\alpha,n} < \epsilon\}}.$$

The two processes are referred as the *large-jump* and the *small-jump* parts, respectively from now on. For the large-jump part, thanks to our assumption that m is finite on $(S, \mathcal{S})$, it is immediately seen that $X_{\epsilon,1}$ has a compound-Poisson representation as

$$\{X_{\epsilon,1}\}_{t\in T} \stackrel{d}{=} \left\{\sum_{j=1}^{N_{\alpha,\epsilon}} V_{\alpha,\epsilon,j} f_t(W_j)\right\}_{t\in T}, \tag{A.3}$$

where N_ϵ is a Poisson random variable with parameter $C_\alpha m(S)\epsilon^{-\alpha}$, W_j are as before, $V_{\alpha,\epsilon,j}$ has probability density $(1/2)\epsilon^\alpha\alpha|y|^{-\alpha-1}, |y| > \epsilon$, and all random variables are independent. An exact simulation of $X_{\epsilon,1}$ in view of (A.3) is straightforward.

The small-jump part $\{X_{\epsilon,2}(t)\}_{t\in T}$ is an infinitely-divisible process that can be approximated by a Gaussian process, as summarized in the following proposition. The proof is essentially the same as Asmussen and Rosiński (2001, Theorem 2.1);

see also Lacaux (2004b, Lemma 4.1) and Cohen et al. (2008, Proposition 5.1). For the sake of completeness we include a proof here again. Let $\nu_\alpha(dx)$ denote the Lévy measure for standard SαS distribution

$$\nu_\alpha(dx) := \frac{\alpha C_\alpha}{2}|x|^{-1-\alpha}dx, x \neq 0.$$

Introduce

$$\sigma_\alpha(\epsilon) := \left(\int_{-\epsilon}^{\epsilon} v^2\nu_\alpha(dv)\right)^{1/2} = \left(\alpha C_\alpha \int_0^\epsilon v^{1-\alpha}dv\right)^{1/2} = \left(\frac{\alpha C_\alpha}{2-\alpha}\right)^{1/2}\epsilon^{1-\alpha/2}.$$

Proposition A.2. *Assume that $f_t \in L^2(S,m)$ for all $t \in T$. Then*

$$\left\{\frac{X_{\epsilon,2}(t)}{\sigma_\alpha(\epsilon)}\right\}_{t\in T} \stackrel{f.d.d.}{\Rightarrow} \{\mathbb{G}(t)\}_{t\in T},$$

as $\epsilon \downarrow 0$, where $\{\mathbb{G}(t)\}_{t\in S}$ is a centered Gaussian process with covariance function

$$\operatorname{Cov}(\mathbb{G}(t_1),\mathbb{G}(t_2)) = \int_S f_{t_1}(s)f_{t_2}(s)m(ds), t_1, t_2 \in T.$$

The tightness of the sequence $\{X_{\varepsilon,2}\}_{\epsilon>0}$ was also established in a few earlier investigated cases (Asmussen and Rosiński, 2001; Lacaux, 2004b). Note that the Gaussian process $\mathbb{G}$ that arises in the limit shares the same form of integral representations as the original SαS process X, with the SαS random measure replaced by a Gaussian random measure ($\alpha = 2$).

Remark A.3. Most examples of interest in Lacaux (2004a,b); Cohen et al. (2008) are such that $S = \mathbb{R}^d$ equipped with the control measure m being the Lebesgue measure. Then, the large-jump part does not have compound–Poisson representation; it is known as a shot-noise model over $\mathbb{R}^d$ in the literature (Vervaat, 1979). Simulating of shot-noise models requires another approximation, with key ideas from Rosiński (2001). On the other hand, the treatment for approximation the small-jump part remains the same for different choices of (S,m). From this point of view, working with a generic (S,m) instead of $(\mathbb{R}^d, \text{Leb})$ as in earlier references does not bring new technical challenges in analysis immediately: choosing m to be finite on S even simplifies our task.

It is worth noting that the assumption on the finiteness on m is not essential, as one could also apply a change-of-measure trick to work with a different representation satisfying this property. The essential constraint here is the L^2-integrability of the functions f_t (after change of measure) that is needed for the Gaussian approximations of the small-jump part (for (A.1) to be a well defined SαS process it suffices to have $f_t \in L^\alpha$ in general). Another notable example of SαS processes that fits into the framework presented here is the one recently introduced in Owada and Samorodnitsky (2015), where S takes a more abstract space than $\mathbb{R}^d$.

Proof of Proposition A.2: We start by providing some background on infinitely-divisble processes. As an infinitely-divisible process, by Samorodnitsky (2016, Theorems 3.3.2 and 3.4.3), (A.2) also can be written as the following integral representation

$$\{X(t)\}_{t\in T} \stackrel{d}{=} \left\{\int_S f_t(s)M_\alpha^{id}(ds)\right\}_{t\in T}, \tag{A.4}$$

where M_α^{id} is an infinitely-divisible random measure on S with control measure dm, and M_α^{id} is uniquely determined by *local characteristics* $\sigma^2 \equiv 0, b \equiv 0, \rho(s,\cdot) = \nu_\alpha(\cdot)$

(Samorodnitsky, 2016, P.86). (The infinitely-divisible random variable $X(t)$ has Lévy measure on $\mathbb{R}$ as the push-forward measure

$$\mu_{f_t} := (m \times \nu_\alpha) \circ T_{f_t}^{-1} \quad \text{with} \quad T_{f_t}(s,x) := x f_t(s), s \in S, x \in \mathbb{R}, \tag{A.5}$$

see Samorodnitsky, 2016, Theorem 3.3.2, although we do not gain anything in this proof by using μ_{f_t}.)

We shall understand stochastic-integral representations as in (A.4) via their corresponding characteristic functions of finite-dimensional distributions based on local characteristics, namely with $\sum_{j=1}^d \theta_j f_{t_j}(s) \equiv g(s)$,

$$\mathbb{E}\exp\left(i\sum_{j=1}^d \theta_j X_{t_j}\right) = \exp\left(\int_S \int_{\mathbb{R}} \left(e^{ig(s)x} - 1 - ig(s)\,[\![x]\!]\right)\nu_\alpha(dx)m(ds)\right), \tag{A.6}$$

where

$$[\![x]\!] = \begin{cases} x & |x| \leqslant 1, \\ -1 & x < 1, \\ 1 & x \geqslant 1. \end{cases}$$

Then, $X_{\epsilon,2}$ has the similar integral representation as (A.4) with M_α^{id} modified by replacing the Lévy measure ν_α by the truncated measure $\mathbf{1}_{\{|v|<\epsilon\}}\nu_\alpha(dv)$. Now we consider for $d \in \mathbb{N}$, $\boldsymbol{t} = (t_1, \dots, t_d) \in T^d$ and $\boldsymbol{\theta} = (\theta_1, \dots, \theta_d) \in \mathbb{R}^d$,

$$g_{\boldsymbol{\theta},\boldsymbol{t}}(s) := \sum_{j=1}^d \theta_j f_{t_j}(s).$$

Then the characteristic function of finite-dimensional distribution of $X_{\epsilon,2}(t)$ is given by (thanks to the symmetry of ν_α, replacing $g(s)\,[\![x]\!]$ in (A.6) by $g(s)x\mathbf{1}_{\{|g(s)x|\leqslant 1\}}$)

$$\mathbb{E}\exp\left(i\frac{\sum_{j=1}^d \theta_j X_{\epsilon,2}(t_j)}{\sigma_\alpha(\epsilon)}\right) = \exp\left(\int_S I_{\alpha,\epsilon}(g_{\boldsymbol{\theta},\boldsymbol{t}}(s))m(ds)\right),$$

with

$$\begin{aligned} I_{\alpha,\epsilon}(y) &:= \int_{\mathbb{R}} \left(\exp\left(i\frac{yx}{\sigma_\alpha(\epsilon)}\right) - 1 - i\frac{y}{\sigma_\alpha(\epsilon)}\,[\![x]\!]\right)\mathbf{1}_{\{|x|\leqslant\epsilon\}}\nu_\alpha(dx) \\ &= \int_{-\epsilon}^{\epsilon} \left(\exp\left(i\frac{yx}{\sigma_\alpha(\epsilon)}\right) - 1 - i\frac{yx}{\sigma_\alpha(\epsilon)}\right)\nu_\alpha(dx), \end{aligned}$$

where we dropped $[\![x]\!]$ on the right-hand side of first line above thanks to the symmetry of ν_α. Now, since $\sigma_\alpha(\epsilon)/\epsilon \to \infty$ as $\epsilon \downarrow 0$, we have

$$I_{\alpha,\epsilon}(y) \sim \int_{-\epsilon}^{\epsilon} -\frac{y^2x^2}{2\sigma_\alpha(\epsilon)^2}\nu_\alpha(dx) = -\frac{y^2}{2}\frac{\int_{-\epsilon}^{\epsilon} x^2\nu_\alpha(dx)}{\sigma_\alpha(\epsilon)^2} = -\frac{y^2}{2}.$$

In addition, for all $y \in \mathbb{R}$, $|I_{\alpha,\epsilon}(y)| \leqslant y^2/2$ (since $|e^{ix} - 1 - ix| \leqslant x^2/2$). Therefore by the dominate convergence theorem we have

$$\begin{aligned} \lim_{\epsilon\downarrow 0}\mathbb{E}\exp\left(i\frac{\sum_{j=1}^d \theta_j X_{\epsilon,2}(t_j)}{\sigma_\alpha(\epsilon)}\right) &= \lim_{\epsilon\downarrow 0}\mathbb{E}\exp\left(\int_S I_{\alpha,\epsilon}(g_{\boldsymbol{\theta},\boldsymbol{t}}(s))m(ds)\right) \\ &= \exp\left(-\frac{1}{2}\int_S |g_{\boldsymbol{\theta},\boldsymbol{t}}(s)|^2\,m(ds)\right). \end{aligned}$$

Now, we read the right-hand side as the the characteristic function of $\sum_{j=1}^{d} \theta_j \mathbb{G}(t_j)$, which completes the proof. $\square$

So for the small-jump part, in practice we shall pick a small number $\epsilon > 0$ and apply the approximation

$$\{X_{\epsilon,2}(t)\}_{t\in T} \approx \{\sigma_\alpha(\epsilon)\mathbb{G}(t)\}_{t\in T}\,,$$

for the corresponding Gaussian process in Proposition A.2. The replacement of small-jump part by a Gaussian process is crucial in view of numerical analysis. For example, for Lévy-driven stochastic differential equations, the performance of approximation schemes is much better with the Gaussian approximation than simply neglecting all the small jumps. See Fournier (2011) and references therein for a detailed investigation.

Remark A.4. As in earlier results, one could also have an Berry–Esseen bound on the pointwise approximation, thanks to Asmussen and Rosiński (2001, Theorem 3.1), Lacaux (2004b, Lemma 4.1): letting

$$s_\epsilon^2(t) = \mathbb{E}X_{\varepsilon,2}^2(t) = \int_S |f_t|^2 dm \int_{-\epsilon}^{\epsilon} x^2 \nu_\alpha(dx) = \mathrm{Var}(\mathbb{G}(t))\sigma_\alpha^2(\epsilon),$$

we have immediately the following rate for the convergence in Proposition A.2 (recall the Lévy measure in (A.5))

$$\begin{aligned}
&\sup_{x\in\mathbb{R}} \left| \mathbb{P}\left(\frac{X_{\varepsilon,2}}{\sigma_\alpha(\epsilon)} \leqslant x\right) - \mathbb{P}(\mathbb{G}(t) \leqslant x) \right| \\
&\qquad \leqslant C_{\mathrm{BE}} \frac{\int_S |f_t|^3 dm \int_{-\epsilon}^{\epsilon} |x|^3 \nu_\alpha(dx)}{s_\epsilon^3(t)} \leqslant C_{\mathrm{BE}} \frac{\int_S |f_t|^3 dm}{(\int_S |f_t|^2 dm)^{3/2}} \frac{(2-\alpha)^{3/2}}{(3-\alpha)\sqrt{\alpha C_\alpha}} \epsilon^{\alpha/2},
\end{aligned}$$

where C_{BE} is the constant in standard Berry–Esseen upper bound for partial sum of centered i.i.d. random variables with unit variance. The value $C_{\mathrm{BE}} = 0.7975$ was used in the aforementioned references, and this value has been improved to 0.4785 in Korolev and Shevtsova (2012).

References

Asmussen, S. and Rosiński, J. Approximations of small jumps of Lévy processes with a view towards simulation. *J. Appl. Probab.*, **38** (2), 482–493 (2001). MR1834755.

Biermé, H. Introduction to random fields and scale invariance. In *Stochastic geometry*, volume 2237 of *Lecture Notes in Math.*, pp. 129–180. Springer, Cham (2019). MR3931585.

Chen, L. H. Y., Goldstein, L., and Shao, Q.-M. *Normal approximation by Stein's method*. Probability and its Applications (New York). Springer, Heidelberg (2011). ISBN 978-3-642-15006-7. MR2732624.

Cohen, S. and Istas, J. *Fractional fields and applications*, volume 73 of *Mathématiques & Applications (Berlin)*. Springer, Heidelberg (2013). ISBN 978-3-642-36738-0; 978-3-642-36739-7. MR3088856.

Cohen, S., Lacaux, C., and Ledoux, M. A general framework for simulation of fractional fields. *Stochastic Process. Appl.*, **118** (9), 1489–1517 (2008). MR2442368.

Cuevas, F., Allard, D., and Porcu, E. Fast and exact simulation of Gaussian random fields defined on the sphere cross time. *Stat. Comput.*, **30** (1), 187–194 (2020). MR4057479.

Dietrich, C. R. and Newsam, G. N. Fast and exact simulation of stationary Gaussian processes through circulant embedding of the covariance matrix. *SIAM J. Sci. Comput.*, **18** (4), 1088–1107 (1997). MR1453559.

Durieu, O., Samorodnitsky, G., and Wang, Y. From infinite urn schemes to self-similar stable processes. *Stochastic Process. Appl.*, **130** (4), 2471–2487 (2020). MR4074708.

Durieu, O. and Wang, Y. From infinite urn schemes to decompositions of self-similar Gaussian process. *Electron. J. Probab.*, **21**, Paper No. 43, 23 (2016). MR3530320.

Fournier, N. Simulation and approximation of Lévy-driven stochastic differential equations. *ESAIM Probab. Stat.*, **15**, 233–248 (2011). MR2870514.

Fu, Z. and Wang, Y. Stable processes with stationary increments parameterized by metric spaces. *J. Theoret. Probab.*, **33** (3), 1737–1754 (2020). MR4125973.

Gelbaum, Z. and Titus, M. Simulation of fractional Brownian surfaces via spectral synthesis on manifolds. *IEEE Trans. Image Process.*, **23** (10), 4383–4388 (2014). MR3300087.

Gnedin, A., Hansen, B., and Pitman, J. Notes on the occupancy problem with infinitely many boxes: general asymptotics and power laws. *Probab. Surv.*, **4**, 146–171 (2007). MR2318403.

Herbin, E. and Merzbach, E. A set-indexed fractional Brownian motion. *J. Theoret. Probab.*, **19** (2), 337–364 (2006). MR2283380.

Herbin, E. and Merzbach, E. The multiparameter fractional Brownian motion. In *Math everywhere*, pp. 93–101. Springer, Berlin (2007). MR2281427.

Istas, J. Spherical and hyperbolic fractional Brownian motion. *Electron. Comm. Probab.*, **10**, 254–262 (2005). MR2198600.

Karlin, S. Central limit theorems for certain infinite urn schemes. *J. Math. Mech.*, **17**, 373–401 (1967). MR0216548.

Korolev, V. and Shevtsova, I. An improvement of the Berry-Esseen inequality with applications to Poisson and mixed Poisson random sums. *Scand. Actuar. J.*, (2), 81–105 (2012). MR2929524.

Kroese, D. P. and Botev, Z. I. Spatial process simulation. In *Stochastic geometry, spatial statistics and random fields*, volume 2120 of *Lecture Notes in Math.*, pp. 369–404. Springer, Cham (2015). MR3330582.

Lacaux, C. Real harmonizable multifractional Lévy motions. *Ann. Inst. H. Poincaré Probab. Statist.*, **40** (3), 259–277 (2004a). MR2060453.

Lacaux, C. Series representation and simulation of multifractional Lévy motions. *Adv. in Appl. Probab.*, **36** (1), 171–197 (2004b). MR2035779.

Lantuéjoul, C. *Geostatistical simulation: models and algorithms.* Springer–Verlag Berlin Heidelberg, first edition (2002). ISBN 978-3-540-42202-0,978-3-642-07582-7,978-3-662-04808-5. DOI: 10.1007/978-3-662-04808-5.

Molchanov, I. *Theory of random sets*, volume 87 of *Probability Theory and Stochastic Modelling.* Springer-Verlag, London (2017). ISBN 978-1-4471-7347-2; 978-1-4471-7349-6. MR3751326.

Owada, T. and Samorodnitsky, G. Functional central limit theorem for heavy tailed stationary infinitely divisible processes generated by conservative flows.

Ann. Probab., **43** (1), 240–285 (2015). MR3298473.

Perrin, E., Harba, R., Jennane, R., and Iribarren, I. Fast and exact synthesis for 1-D fractional Brownian motion and fractional Gaussian noises. *IEEE Signal Processing Letters*, **9** (11), 382–384 (2002). DOI: 10.1109/LSP.2002.805311.

Pitman, J. *Combinatorial stochastic processes*, volume 1875 of *Lecture Notes in Mathematics*. Springer-Verlag, Berlin (2006). ISBN 978-3-540-30990-1; 3-540-30990-X. MR2245368.

Rosiński, J. Series representations of Lévy processes from the perspective of point processes. In *Lévy processes*, pp. 401–415. Birkhäuser Boston, Boston, MA (2001). MR1833707.

Samorodnitsky, G. *Stochastic processes and long range dependence*. Springer Series in Operations Research and Financial Engineering. Springer, Cham (2016). ISBN 978-3-319-45574-7; 978-3-319-45575-4. MR3561100.

Samorodnitsky, G. and Taqqu, M. S. *Stable non-Gaussian random processes. Stochastic models with infinite variance*. Stochastic Modeling. Chapman & Hall, New York (1994). ISBN 0-412-05171-0. MR1280932.

Schneider, R. and Weil, W. *Stochastic and integral geometry*. Probability and its Applications (New York). Springer-Verlag, Berlin (2008). ISBN 978-3-540-78858-4. MR2455326.

Sibuya, M. Generalized hypergeometric, digamma and trigamma distributions. *Ann. Inst. Statist. Math.*, **31** (3), 373–390 (1979). MR574816.

Stein, M. L. Fast and exact simulation of fractional Brownian surfaces. *J. Comput. Graph. Statist.*, **11** (3), 587–599 (2002). MR1938447.

Takenaka, S. Stable random fields and geometry. In *Stability in probability*, volume 90 of *Banach Center Publ.*, pp. 225–241. Polish Acad. Sci. Inst. Math., Warsaw (2010). MR2798862.

van Wyk, H.-W., Gunzburger, M., Burkhardt, J., and Stoyanov, M. Power-law noises over general spatial domains and on nonstandard meshes. *SIAM/ASA J. Uncertain. Quantif.*, **3** (1), 296–319 (2015). MR3338005.

Vervaat, W. On a stochastic difference equation and a representation of nonnegative infinitely divisible random variables. *Adv. in Appl. Probab.*, **11** (4), 750–783 (1979). MR544194.

Wood, A. T. A. and Chan, G. Simulation of stationary Gaussian processes in $[0,1]^d$. *J. Comput. Graph. Statist.*, **3** (4), 409–432 (1994). MR1323050.